PHYSICAL REVIEW B VOLUME 43, NUMBER 10 1 APRIL 1991

Langevin molecular dynamics of interfaces: Nucleation versus spiral growth

F. Falo,* A. R. Bishop, and P. S. Lomdahl
Theoretical Division and Advanced Computing Laboratory, Los Alamos National Laboratory, Los Alamos, New Mexico 87545

B. Horovitz
Physics Department, Ben-Gurion University, Beer Sheva 84105, Israel
(Received 15 October 1990)

A simulation of surface growth is reported that directly introduces dynamics and thermal noise within a classical Langevin molecular-dynamics scheme. Using recent advances in massively parallel computation, extensive simulations on large two-dimensional lattices are possible. Surface growth is modeled by a dynamic solid-on-solid model, analogous to a discrete two-dimensional sine-Gordon equation. The influence of both homogeneous (thermal) nucleation and Frank-Read sources of spiral growth patterns are incorporated and compared. A phase diagram is described in the space of temperature and chemical potential difference between surface and vapor. At sufficiently high temperatures, a surface-roughening transition occurs. Finally, the same model is applied to other two-dimensional contexts: charge-density-wave materials in an electric field, and a two-dimensional Josephson junction in a perpendicular current.

I. INTRODUCTION

The role of coherent localized and extended defects such as vortices, dislocations, domain walls, grain boundaries, etc., in the dynamical properties of materials is an interesting and fascinating subject which is not yet very well understood. These kinds of defects play important roles in modifying both equilibrium (e.g., strength) and nonequilibrium (e.g., response) properties of materials.

This paper is devoted to the simulation of *spiral growth* patterns produced by the existence of dislocation defects, as an important example of coherent structures. Such patterns appear in different fields of nonlinear science. Here, we analyze their influence on several dynamical properties in the context of the two-dimensional (2D) discrete sine-Gordon equation which can model various physical systems. For instance, "whisker" crystal-growth dynamics has been shown to be an excellent example of this behavior, and extensively studied experimentally and theoretically. Spiral growth from Frank-Read (FR) sources (two emergent screw dislocation in the surface) was early predicted theoretically.[1] Monte Carlo (MC) simulations supported the validity of such a scenario.[2] This FR dynamical mechanism has also been suggested for the depinning of charge-density waves (CDW) by an electric field.[3] Here dislocations with opposite Burgers vectors in the CDW lattice form a FR source and facilitate charge flow. On the other hand, reaction-diffusion systems are examples of systems exhibiting similar self-organizing structures. For example, inorganic reactions (such as the Belousov-Zhabotinskii reaction) and enzyme-catalyzed reactions show periodic behavior strongly related with the appearance of spatial structures and the formation of spiral waves.[4]

Our aim here is to use Langevin molecular dynamics to directly simulate the dynamic processes without the artificial time steps inherent in MC schemes. Advances in computational techniques discussed below now allow access to nonequilibrium processes at finite temperature on systems of substantial size.

Dynamic problems couched in the language of the 2D sine-Gordon system lend themselves to a very easy and efficient implementation on novel parallel computer architectures of the fine-grained SIMD (single instruction multiple data) type, like the Connection Machine 2. There are several reasons for this: First, large systems are necessary to obtain good statistics for temperature-dependent phenomena; second, interactions are often local in nature with only nearest- or next-nearest-neighbor interactions, which makes the communication topology between processors very simple. We have implemented a set of stochastic Runge-Kutta methods, proposed by Greenside and Helfand[5] to integrate nonlinear Langevin equations in a code, SLaP (Simplified Langevin Programming), which runs on the Connection Machine 2(CM-2). The performance is very good (approximately 300 MFlops on a 16000 processor CM-2) and it allows us to study large systems (e.g., 512×512 square lattices) with only 10–15 min CPU time per run. We have applied SLaP in our study of spiral growth reported here, but the code is quite flexible and application to other problems (e.g., large arrays of Josephson junctions) is in progress and will be reported elsewhere.

The structure of this paper is as follows: In Sec. II, we introduce our model for spiral growth dynamics and the Langevin MD simulation procedure. Derivations in the context of surface physics, charge-density waves, and Josephson junctions are outlined. In Sec. III we show different dynamical regimes for growth (spiral or nucleation) and discuss the crossover between them. An estimation of the roughening transition temperature is obtained in Sec. IV. Finally, a dynamical "phase diagram" is proposed and discussed in Sec. V.

II. EQUATION OF MOTION

A. Crystal growth

We use as an example for the simulation of spiral patterns the phenomenon of crystal growth. Crystal surface processes have been modeled by so-called "solid-on-solid" (SOS) models in which one considers a *discrete* integer variable h_i, representing the height of the column i over a flat surface. The energy of interaction between columns is given generally by

$$E=\sum_{\langle i,j\rangle} F(h_i-h_j)\ . \tag{1}$$

Here F is an arbitrary function and the summation extends over nearest neighbors. Burton, Cabrera, and Frank[1] introduced this model with $F(x)=|x|$ and $h_i=0$ or 1. With this choice, the Hamiltonian (1) is equivalent to an Ising model and a roughening transition occurs with temperature which has Ising character. A more general (and still solvable) possibility is to allow the variable h_i to take all integer values and to consider the interaction $F(x)=x^2$. This is called the "discrete Gaussian SOS" (DGSOS) model and has interesting implications. Some time ago, it was shown[6] that this model is dual to the planar XY magnet and neutral Coulomb gas models, as far as equilibrium properties are concerned. This means that the roughening transition is of Kosterlitz-Thouless type—i.e., driven by vortex-antivortex unbinding rather than discrete symmetry breaking as in the Ising case. A considerable body of work has been developed studying the static and MC dynamical properties of this model. (See, e.g., Ref. 7.)

As a way to study the nonequilibrium *dynamics* in the DGSOS model we consider the modified Hamiltonian[8]

$$H=\tfrac{1}{2}\sum_{\langle i,j\rangle}(\phi_i-\phi_j)^2-\sum_i\cos(\phi_i)+I\sum_i\phi_i\ , \tag{1a}$$

with ϕ a continuous variable. The second term in (1a) favors ϕ_i to be $2\pi n$ (n integer), so we can make the identification $\phi=2\pi h$. The last term is a uniform driving force which corresponds to the chemical potential difference between the surface and the vapor. The Hamiltonian (1a) is nothing but the discrete version of the driven sine-Gordon equation in two space dimensions, i.e., the two-dimensional Frenkel-Kontorova model. The Langevin equations of classical motion for ϕ following from (1a) read

$$\begin{aligned}&\ddot{\phi}_i-\epsilon\dot{\phi}_i=\sum_\eta(\phi_{i+\eta}-\phi_i)+\sin(\phi_i)+I+\xi_i(t)\ ,\\ &\langle\xi_i(t)\rangle=0,\quad\langle\xi_i(t)\xi_j(t')\rangle=2\epsilon T\delta(t-t')\delta_{ij}\ ,\end{aligned} \tag{2}$$

Where η runs over nearest neighbors, $\epsilon\dot{\phi}$ is a damping term (ϵ can be identified with the equilibrium evaporation rate[7]), and $\xi_i(t)$ is thermal white noise which couples the system to a heat bath at temperature T (in units of k_B). Note that using this Hamiltonian our temperature units are $4\pi^2$ times ones often used in the literature.[8,9] The continuous, static ($\dot{\phi}=0, I=0$) equation following from (2) is $\nabla^2\phi=\sin\phi$. This has, for example, one-dimensional domain wall solutions and approximate spherical cluster ones.

We are also interested in the dynamics of a surface in the presence of emergent screw dislocations which play an important role in whisker crystal-growth mechanisms. A screw dislocation is given approximately by

$$\phi_0(x,y)=\tan^{-1}\left[\frac{y}{x}\right]\ , \tag{3}$$

where x,y are the Cartesian coordinates in the continuum limit. However, this function is not a solution of the static undriven sine-Gordon equation so it is not a suitable initial condition for the equations of motion (2). (The dislocation is not a static solution, which is not physically acceptable.) We can simulate the presence of the dislocation configuration by forcing the surface ϕ to grow *relative* to the dislocation ϕ_0, i.e., replacing $\phi(r,t)$ by $[\phi(r,t)-\phi_0(r)]$ in the sine term of equation of motion. This results in the following modified equation of motion:

$$\ddot{\phi}_i-\epsilon\dot{\phi}_i=\sum_\eta(\phi_{i+\eta}-\phi_i)+\sin(\phi_i-\phi_{0i})+I+\xi_i(t)\ . \tag{4}$$

Now the static equation is $\nabla^2\phi=\sin(\phi-\phi_0)$. In our simulation of Eq. (4), we have used for ϕ_0 the function representing a *pair* of fixed screw dislocations with opposite Burger vectors, i.e., a Frank-Read source for crystal growth.

B. Josephson junction and CDW

Here we derive our equation of motion for either flat or spiral surface growth in the context of two other types of systems—Josephson junctions, and CDW dynamics.

Consider first the case of a Josephson junction centered at a plane $z=0$ separating two bulk superconductors. A "flat" boundary corresponds to boundary conditions with currents $J_x, J_y\to 0$ far from the junction, i.e., magnetic fields are parallel to the junction and are confined to be near the junction by Meissner currents. A "spiral" boundary allows for a pair of opposite flux lines to penetrate the junction from one side, say $z>0$. The boundary condition for $x\to-\infty$ is a flat one while $x\to\infty$ the phase $\phi(x,y,z)$ of the order parameter approaches

$$\phi_b(x,y)=\tan^{-1}\left[\frac{y}{x-x_0}\right]-\tan^{-1}\left[\frac{y}{x+x_0}\right]\ , \tag{5}$$

so that $\oint\nabla\phi_b(x,y)\cdot dl=\pm 2\pi$ with the integral circling in the x,y plane around each vortex at $(\pm x_0,0)$.

We now rederive Josephson's equation[10] for these boundary conditions. The free energy of each superconductor is given by

$$F=\int d^3r[\mathbf{h}^2/8\pi+(\hbar^2/2m)n_s(\nabla\phi-2eA/\hbar c)^2]\ , \tag{6}$$

where $\mathbf{h}(\mathbf{r})=\nabla\times\mathbf{A}$ is the internal magnetic field, n_s is the density of superconducting electrons, and $\mathbf{A}$ is the electromagnetic vector potential. The equation for the current $\mathbf{J}$ follows from $\delta F/\delta\mathbf{A}=0$, i.e.,

$$\mathbf{J}=(c/4\pi)\nabla\times\mathbf{h}=(e\hbar/2m)n_s(\nabla\phi-2e\,\mathbf{A}/\hbar c)\ . \tag{7}$$

The Josephson phase $\phi_J(x,y)$ contains a nonsingular function $\phi(x,y)$ as well as the singular part $\phi_b(x,y)$, where

$$\phi(x,y)=\phi(x,y,\infty)-\phi(x,y,-\infty)\ ,$$
$$\phi_J(x,y)=\phi(x,y)+\phi_b(x,y)\ . \tag{8}$$

The boundary conditions for the currents J_x,J_y in Eq. (7) correspond to

$$\nabla\phi(x,y,z)-2e\,\mathbf{A}/\hbar c=\begin{cases}\nabla\phi_b(x,y), & z\to+\infty\ ,\\ 0, & z\to-\infty\ .\end{cases} \tag{9}$$

Consider an area perpendicular to y with width dx in the x direction and extending to $\pm\infty$ in the z direction. Choosing a gauge $A_z=0$, the flux through this area can be written in the form

$$\begin{aligned}h_y^{\rm av}(x,y)dx &\equiv dx\int_{-\infty}^{\infty}h_y(x,y,z)dz\\ &=\oint\mathbf{A}\cdot d\mathbf{l}=[A_x(x,y,\infty)-A_x(x,y,-\infty)]dx\\ &=dx(\hbar c/2e)\frac{\partial}{\partial x}[\phi(x,y)-\phi_b(x,y)]\ .\end{aligned} \tag{10}$$

A similar equation follows for $h_x^{\rm av}(x,y)$, i.e., $h_x(x,y,z)$ integrated on z. Thus the z dependence can be eliminated by using the integrated 2D fields $\mathbf{h}^{\rm av}=(h_x^{\rm av},h_y^{\rm av})$ for which

$$\mathbf{h}^{\rm av}(x,y)=(\hbar c/2e)\hat{\mathbf{z}}\times\nabla[\phi(x,y)-\phi_b(x,y)]\ , \tag{11}$$

where $\hat{\mathbf{z}}$ is a unit vector normal to the junction.

The z component of the equation of motion, Eq. (7), becomes

$$\begin{aligned}(c/4\pi)[-\partial_y h_x(x,yz)+\partial_x h_y(x,y,z)]\\ =(e\hbar/2m)n_s\frac{\partial\phi(x,y,z)}{\partial z}\ .\end{aligned} \tag{12}$$

Integrating z yields the Josephson phase $\phi(x,y)$ on the right-hand side. The junction effect[10] is to replace ϕ_J by $\sim\sin\phi_J$, so that observables are periodic in ϕ and spatial variations in ϕ are important only where $\phi\neq 2\pi$. Substituting (10) into the z integrated (12) and use of $\phi_J(x,y)$ [Eq. (8)] finally yields

$$\nabla^2\phi(x,y)=(1/\lambda_J)^2\sin[\phi(x,y)+\phi_b(x,y)]\ , \tag{13}$$

where λ_J is the Josephson penetration length. Note that no assumption on an exponential decay of $\mathbf{h}(x,y,z)$ in the z direction (as in usual derivations[10]) has been made.

We consider next the CDW problem in which the phenomena of a sliding CDW and generation of current oscillations by a dc field have been associated with the formation of dislocations,[3,11] vortices,[12] or phase slip defects.[13] Matching of a sliding CDW with a static one near an external contact[12] defines a plane which, as demonstrated below, acts as a Josephson junction.

A CDW describes density modulations of the form $\cos[\mathbf{q}\cdot\mathbf{r}+\phi(\mathbf{r})]$ with $\mathbf{r}=(x,y,z)$ and q_z incommensurate with the underlying lattice, so that sliding in the z direction due to an external force is relatively easy. The elastic energy due to phase deformations is[3,14]

$$F=\tfrac{1}{2}\epsilon_0\int d^3r'[\nabla_{r'}\phi(r')]^2\ , \tag{14}$$

where $r_{1'}=x/\xi_x$, $r_{2'}=y/\xi_y$, $r_{3'}=z/\xi_z$, with $\xi_z=v_F/\Delta$, $\xi_x\cong\xi_y$, are transverse coherence lengths, $\epsilon_0=\Delta^2\xi_x\xi_y\xi_z/\epsilon_F b^2 a$, v_F is the Fermi velocity, ϵ_F is the Fermi energy, Δ is the gap in the electron spectrum, a is the lattice constant in the z direction, and b^2a is the volume of the unit cell.

The energy (14) has to be supplemented by the presence of dislocations-defect lines around which $\oint\nabla\phi(\mathbf{r})\cdot d\mathbf{l}=\pm 2\pi$. Since the CDW is periodic only in one direction it restricts Burgers vectors to be parallel to $\mathbf{q}$; the corresponding dislocations are either screw or edge type.[3,11] We consider a "junction" on a plane perpendicular to $\mathbf{q}$, between two CDW formations; one is, say, sliding and the other static. The junction plane can have many dislocation loops, yet there are paths across the junction which favor the phase difference across the junction [Eq. (8)] to be a multiple of 2π. This nonlocal effect results in a coupling which is periodic in $\phi(x,y)$, as in Eq. (13).

A more quantitative derivation follows the route of He^4, an equivalent system with a complex order parameter. The He^4 problem has been shown[15] to be equivalent to that of charged particles coupled to a gauge field $\mathbf{a}(\mathbf{r})$. The related XY model on a lattice has also been transformed into a gauge theory[16,17] which in terms of a disorder field $\psi=|\psi|e^{i\gamma}$ has the form[17]

$$F_1=\int d^3r'\{\tfrac{1}{2}|\nabla_{r'}\gamma(r')-e^*\mathbf{a}(\mathbf{r}')|^2+\tfrac{1}{2}[\nabla_{r'}\times\mathbf{a}(\mathbf{r}')]^2\} \tag{15}$$

assuming a constant $|\psi|$.

The CDW problem is now formally equivalent to that of Eq. (2) with the temperature $T^*=\epsilon_0/T$ for the superconductor Eq. (15) and the charge $e^*=2\sqrt{\pi}$. The line singularities of $\nabla\times\nabla\phi$ in the CDW problem correspond to line singularities of $\nabla\times(\nabla\gamma-e^*\mathbf{a})$ and hence to magnetic flux lines in the superconductors. Flat boundaries correspond then to no dislocations far from the junction, while spiral boundaries correspond to a pair of screw dislocations parallel to $\hat{\mathbf{z}}$. The latter case is precisely the Frank-Read source for generation of dislocation loops in the junction plane.[3]

Repeating the steps in Eqs. (3)–(9) we obtain

$$\nabla^2\gamma(x,y)=(1/\lambda^*)^2\sin[\gamma(x,y)+\phi_b(x,y)]\ , \tag{16}$$

where $\lambda^{*2}=\xi_x^2/e^{*2}$. Equations (13) and (16) show that the static equation for crystal growth is equivalent to that of a Josephson junction and of a CDW "junction." We next propose that the dynamics of these systems is given by Eq. (4).

The force I and the growth rate $\langle\dot\phi\rangle$ ($\langle\ \rangle$ denotes space average) have different interpretations in the three systems. For the Josephson junction case I and $\langle\dot\phi\rangle$ are the current density and voltage across the junction, respectively. In the CDW case I is the electric field while $\langle\dot\phi\rangle$ is the current carried by the sliding CDW. The actual transformation to Eq. (15) in presence of I is not obvious since its energy $I\,\phi(\mathbf{r})$ is unbounded; instead we use the

analogy of $\nabla\gamma - e^*\mathbf{a}$ with $\nabla\phi$ to obtain a force I in Eq. (16). As for the original ϕ equation[3] the free energy which corresponds to (16) involves an energy scale (analogous to the Josephson current) which requires a separate calculation. Finally, in the crystal-growth problem I is the solid-vapor chemical potential difference and $\dot{\phi}$ is the growth rate of the surface.

III. SPIRAL GROWTH DYNAMICS

Direct simulation of equations (4) gives clear evidence of the Frank-Read source mechanism for crystal growth. Figure 1(a) shows snapshots from the time evolution of the initial condition: a pair of screw dislocations given by Eq. (5). Here, the separation between dislocations ($2x_0$) is 100 lattice units and $I=0.8$. Figure 1(b) shows snapshots from the time evolution of the growth rate ($\dot{\phi}$): The spiral growth is especially clear. Finally, Fig. 1(c) shows snapshots from the time evolution of a simulation at finite temperature ($T=1.0, I=0.65$): In this case spiral growth is still present, but homogeneous nucleation is also beginning to appear. At a slightly higher temperature nucleation dominates the growth process. According to the Cabrera and Levine *continuum* theory[1] for

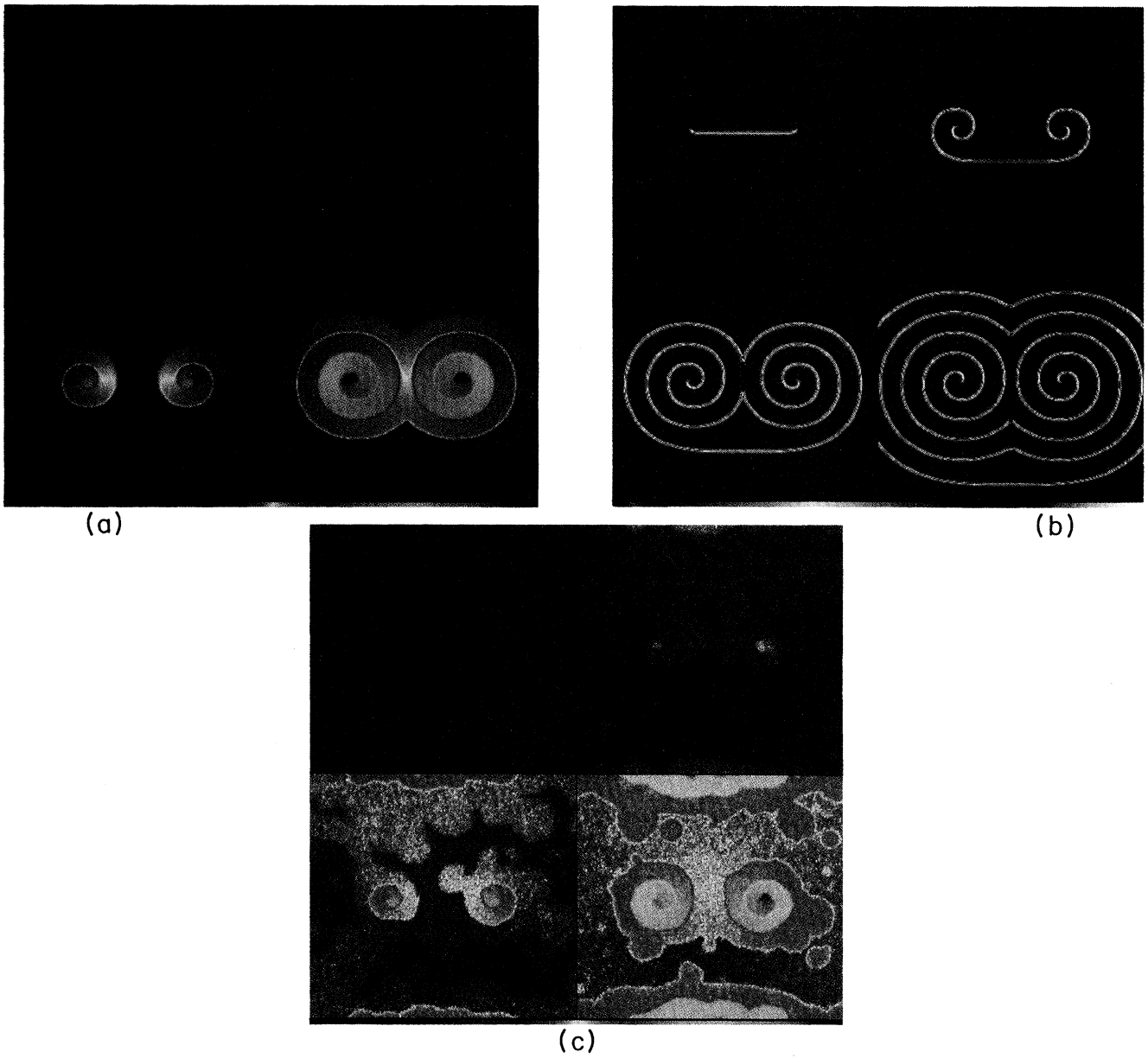

FIG. 1. Snapshots from the time evolution of two counter rotating spirals (a Frank-Read source). Panels (a), where $I=0.8$, $\epsilon=1.0$, and $T=0$, show ϕ for four different time snapshots. Panels (b) show the growth rate $\dot{\phi}$ for the same parameter values. Finally panels (c) show the growth of ϕ at a finite temperature just below the crossover to nucleation dominated growth ($I=0.65$, $\epsilon=1.0$, and $T=1.0$). Note in addition to the spiral a large nucleation cluster near the (periodic) boundary. The times are the same as for panels (a) and (b). The color bar at the bottom of each panel gives the magnitude of the growth (growth rate) increasing from left to right.

overdamped spiral growth, the radial velocity of the step and the (the inverse of the) separation between spiral arms are proportional at large distances to the supersaturation, i.e., to I, if the separation $2x_0 \gg$ the spiral arm spacing. Then the surface growth rate ($V = \langle\langle \dot{\phi} \rangle\rangle$) is expected to be proportional to I^2. We have calculated the growth rate [see Fig. 2(a)] and find good agreement with this prediction. For x_0 smaller than the spiral arm separation we find a clear deviation from this behavior. Figure 3 shows the spiral arm separation versus I for several *small* values of x_0. For $2x_0 = 5$ the curve is close to the continuum limit. For lower values of the dislocation separation we find higher critical fields I which is also in agreement with theory, i.e., $2x_0 \gg \rho_c$, ρ_c being the critical nucleation radius.

From Fig. 2(a) it is possible to identify the "crossover" between spiral and nucleation dominated regimes. The nucleation growth rate can be obtained by using a flat surface [dotted lines in Fig. 2(a)]. The difference in growth rates between both initial conditions is shown in Fig. 2(b). At temperature $T=0$, the crossover is at $I=1$ in which the whole surface grows uniformly. (In fact, at $T=0$ the whole system behaves like a single point Josephson junction.) At finite temperatures, the crossover region broadens and shifts to lower I, disappearing at $T \simeq 6$. On the other hand, the spiral mechanism dramatically reduces the critical force I_c with respect to the pure nucleation processes. The critical force I_c depends on several factors; first (as we have seen above) on the separation of dislocations; second, on lattice discreteness (which provides an intrinsic Peierls-Nabarro pinning); and finally on the temperature. In fact, the very concept of I_c is not well defined in numerical simulation (as in real experiments) since it is limited by finite observation time. For very low forces ($I < 0.1$) the dynamics can be so slow and only very long time simulations distinguish between pinned and slowly moving configuration. In any case, we have been able to determine $0.05 < I_c < 0.1$ for spiral growth for $T=0$ in contrast with $I_c \simeq 1$ for the flat surface.

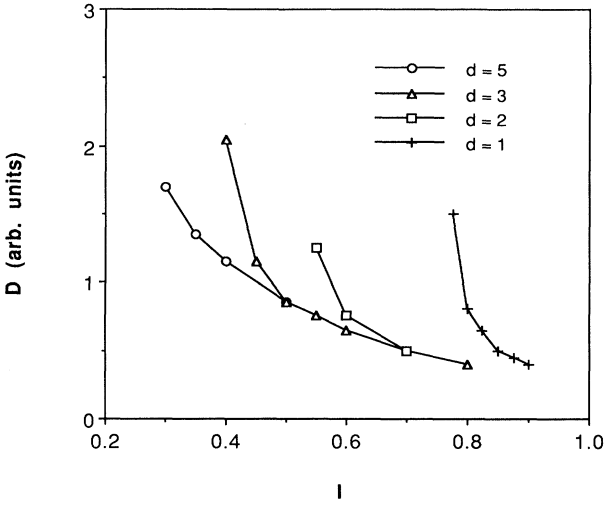

FIG. 3. Spiral arm separation (D) vs I for different values of the distance between screw dislocations ($2x_0 = d$).

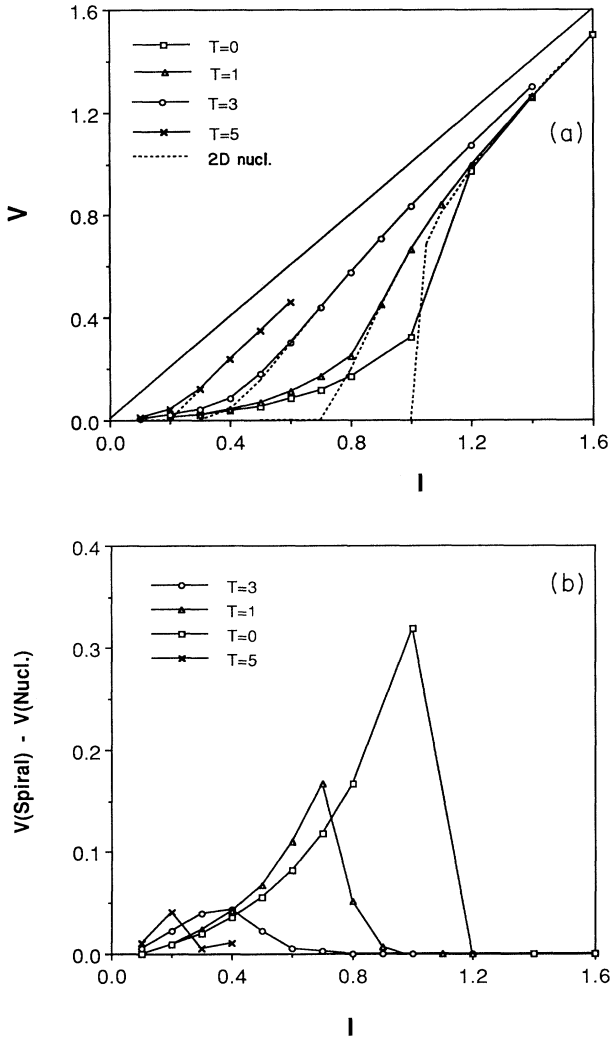

FIG. 2. (a) Growth rate average (V) vs I for different temperatures using a Franck-Read source (solid lines) and flat surface (dotted line) as initial conditions, respectively; (b) difference in V between the two growth mechanisms.

Another interesting dynamical feature is the behavior of $\langle \dot{\phi}(t) \rangle$ in the two growth regimes. Figure 4 shows $\langle \dot{\phi}(t) \rangle$ at $T=0$ for $I=0.5$ (spiral growth) and $I=1.2$ (nucleation growth). In the spiral growth regime, a clear periodic behavior is observed with peaks corresponding to periodic formation and annihilation of new layers at the Frank-Read source and boundaries, respectively. The frequency of the signal fulfills the Josephson relation $\omega = \langle\langle \dot{\phi} \rangle\rangle$ and therefore it is proportional to I^2. This frequency corresponds to the generation of the new spirals which controls the voltage oscillations. This scenario breaks down near the crossover with the nucleation regime where a high-frequency pattern corresponding to the space-uniform ac Josephson effect appears. Figure 5 shows the time series at finite temperatures. In spite of the thermal noise a similar structure is again observed

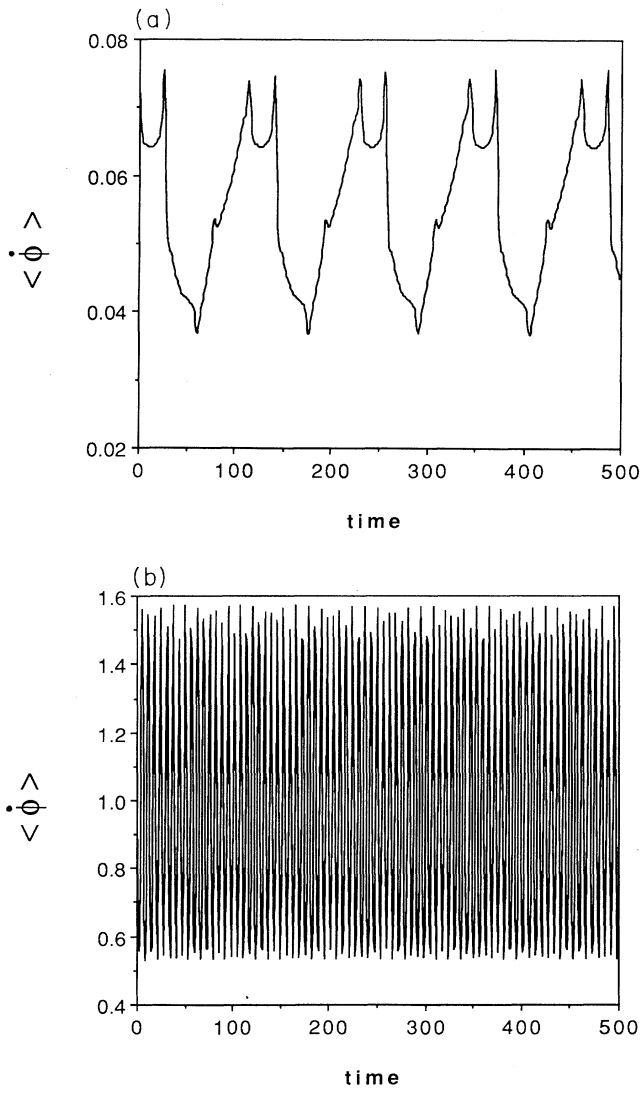

FIG. 4. (a) $\langle \dot{\phi}(t) \rangle$ vs time at $T=0$ in the spiral growth regime; (b) the same as (a) but in the nucleation regime.

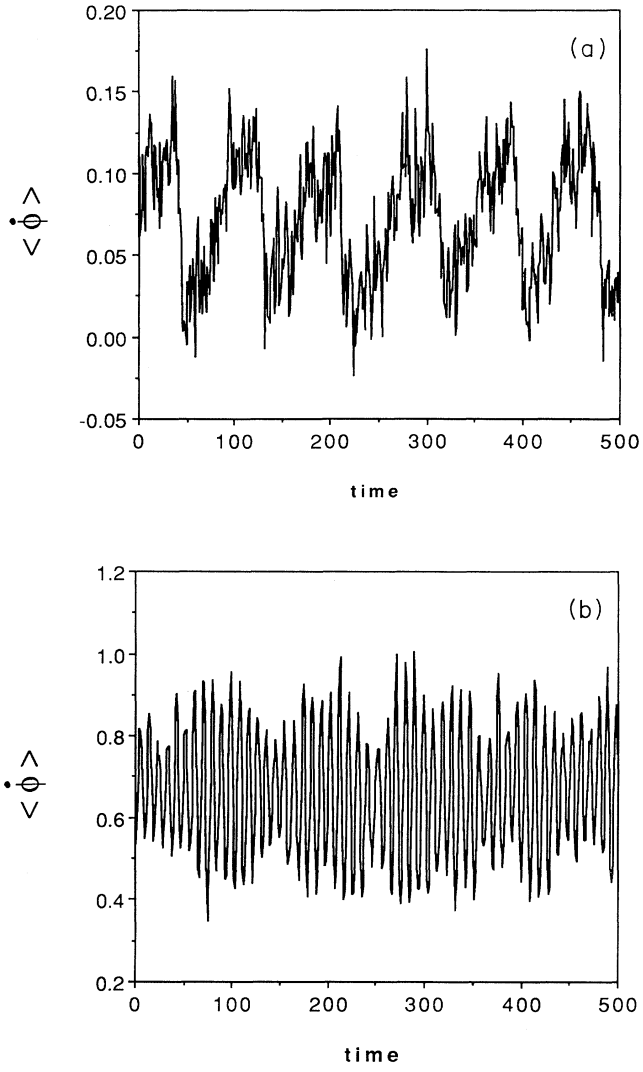

FIG. 5. (a) $\langle \dot{\phi}(t) \rangle$ vs time at $T=1.0$ in the spiral growth regime; (b) the same as (a) but in the nucleation regime.

giving a signature of the crossover region.

In the underdamped regime ($\epsilon \ll 1$) the dynamics is substantially more complicated, but spiral growth is still possible. For instance, for $\epsilon=0.1$ we have found that the dynamics leads to irregular shapes of emerging rings generated by the spiral growth. This is due in part to the complicated dynamics during the collision of two counter rotating spirals which, in the underdamped case, is more like a regular sine-Gordon kink-antikink collision, while the overdamped dynamics behaves more like an annihilation process.

IV. ROUGHENING TRANSITION

For high fields and/or high temperatures, nucleation processes dominate and the presence of the dislocations is unimportant (although we have observed that they act as preferential nucleation regions). For high enough temperature the surface melts in the sense there is no energy cost to create steps (i.e., there is a roughening transition). According to the duality mapping between DGSOS model and XY models for $I=0$, this transition at temperature T_R should have a Kosterlitz-Thouless (KT) character. In fact, renormalization group (RG) recursion equations for Hamiltonian (1) ($I=0$) are the same as the KT ones. One way to locate the transition temperature is to investigate the height-height correlation function given by[9]

$$C(r)=\langle [\phi(0)-\phi(r)]^2 \rangle \ . \tag{17a}$$

For $T > T_R$ and $I=0$ the cosine term in the Hamiltonian (1a) is irrelevant under renormalization, and therefore reduces to a pure 2D Gaussian model behavior. Thus the correlation function becomes[7]

$$C(r)=\frac{A(T)}{\pi}\ln(r)=2\eta(T)\ln((r) \ , \tag{17b}$$

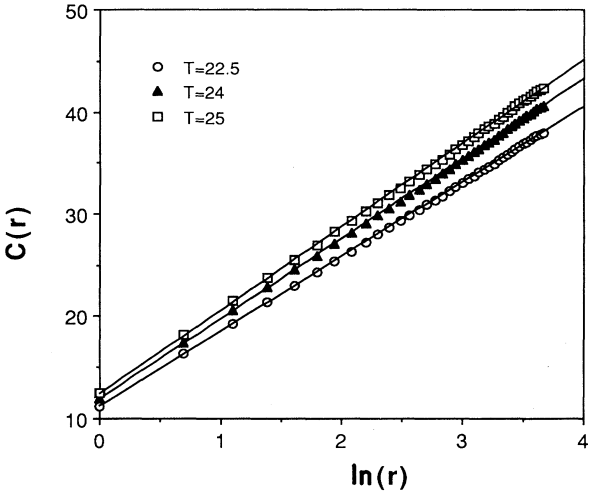

FIG. 6. Log-linear fit of the correlation function [Eq. (17a)]. The slopes are 7.31, 7.83, and 8.17 for $T=22.5$, 24, and 25, respectively.

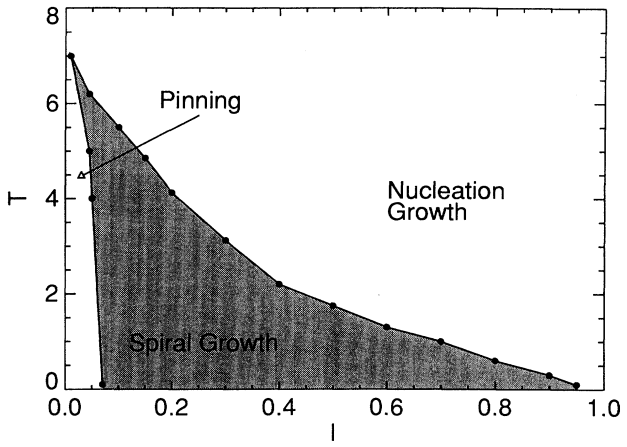

FIG. 7. Semischematic phase diagram, showing spiral growth, nucleation, discreteness pinned, and melted regimes.

where $A(t)$ is a function of temperature. Below T_R, we have a finite correlation length ξ and the correlation function is

$$C(r)=\frac{1}{2\pi}A(T)\ln[(r^{-2}+\xi^{-2})]^{-1}\ . \tag{17c}$$

Thus, for $R\to\infty$, $C(r)\approx\ln\xi$. We can use the RG expectations[9] that $A(T_R)=8\pi$ in our variables and is a universal quantity. Figure 6 shows the correlation function for temperatures near our numerically estimated $T_R=24.5$. For finite systems the crossover between forms (17b) and (17c) is smooth; this estimation has been made by using the universal value $\eta(T_R)=4$. RG analysis for the continuum model gives $T_R=8\pi\approx25.13$, in fair agreement with our numerical results.

V. DISCUSSION

We can summarize the foregoing results in a schematic phase diagram (Fig. 7) for the different dynamical regimes. As we have described in Sec. II, the presence of dislocation-like defects dramatically changes the dynamics at low temperatures and driving forces. Several regions are well defined in the presence of such defects: A spiral growth mechanism is developed—strongly decreasing the critical field for surface growth. A crossover between spiral and nucleation growth is obtained with increasing temperatures for $I<1$.

Different condensed matter systems can exhibit the kind of dynamics we have discussed. For instance, dislocations in a charge-density-wave lattice can act as a Frank-Read source giving a reduced value for the critical electric depinning field. A similar mechanism can be invoked in thin film superconductors or large Josephson junctions for flux motion. The dynamics of the spiral growth regime is characterized by the nonlinear behavior $\langle\langle\dot{\phi}\rangle\rangle\approx I^2$ which should be experimentally accessible. At finite temperature the crossover broadens but it is still possible to distinguish both spiral and nucleation mechanisms. Below the equilibrium roughening temperature T_R and in the nucleation regime, the growth rate is given by $\langle\langle\dot{\phi}\rangle\rangle\approx\exp(-c/I)$. Above T_R a linear behavior ($\langle\langle\dot{\phi}\rangle\rangle\approx I$) has been found as predicted in RG theory.[8]

In conclusion, we have studied a model which can simulate spiral and nucleative growth patterns. We have calculated dynamical properties of this model using a Langevin MD method obtaining, in a dynamical sense, the phase diagram for crystal growth. The great variety of systems which present this kind of coherence structure leads us to expect that new applications will occur in such different fields as material science, chemistry, and biology. Furthermore, the opportunity to study these processes with Langevin MD rather than MC techniques is now greatly enhanced because of access to massively parallel computing capabilities like the CM-2. We believe that a synergistic combination of large-scale computing and techniques from nonlinear science opens qualitatively new opportunities to study nontrivial microscopic dynamical processes and their relation to macroscopic response properties.

ACKNOWLEDGMENTS

One of us (P.S.L.) would like to thank Terry Dontje and Eugene Loh of Thinking Machines Corporation for their support. We also thank the Los Alamos Advanced Computing Laboratory for providing access to the CM-2. F.F. acknowledges the Theoretical Division and Advanced Computing Laboratory at Los Alamos National Laboratory (LANL) for its hospitality. B.H. would like to thank J. Adler and S. A. Brazovski for stimulating discussions. This work was supported at Los Alamos National Laboratory by the U.S. Department of Energy (USDOE).

*Permanent address: Departamento de Ciencia y Tecnologia de Materiales y Fluidos and Instituto de Ciencia de Materiales de Aragon, Universidad de Zaragoza, C.S.I.C., 50009 Zaragoza, Spain.

[1]F. C. Frank and W. T. Read, Phys. Rev. **79**, 722 (1950); W. K. Burton, N. Cabrera, and F. C. Frank, Philos. Trans. R. Soc. London **243A**, 299 (1951); N. Cabrera and M. M. Levine, Philos. Mag. **1**, 450 (1956).

[2]R. H. Swendsen, P. J. Kortman, D. P. Landau, and H. Muller-Krumbhaar, J. Cryst. Growth **35**, 73 (1976); G. H. Gilmer, *ibid.* **36**, 15 (1976).

[3]P. A. Lee and T. M. Rice, Phys. Rev. B **19**, 3970 (1979).

[4]See, e.g., G. Nicolis and I. Pigogine, *Self-organization in non-equilibrium systems* (Wiley, New York, 1977).

[5]H. S. Greenside and E. Helfand, Bell Syst. Tech. J. **60**, 1927 (1981).

[6]J. V. José, L. P. Kadanoff, S. Kirkpartick, and D. R. Nelson, Phys. Rev. B **16**, 1217 (1977); H. J. F. Knops, Phys. Rev. Lett. **39**, 776 (1977).

[7]J. D. Weeks and G. H. Gilmer, Adv. Chem. Phys. **40**, 157 (1979).

[8]S. T. Chui and J. D. Weeks, Phys. Rev. Lett. **40**, 157 (1979).

[9]W. J. Shugard, J. D. Weeks, and G. H. Gilmer, Phys. Rev. Lett. **41**, 1399 (1978).

[10]B. D. Josephson, Adv. Phys. **14**, 419 (1965); M. Tinkham, *Introduction to Superconductivity* (McGraw-Hill, New York, 1975).

[11]D. Feinberg and J. Friedel, J. Phys. (Paris) **49**, 485 (1988).

[12]N. P. Ong and K. Maki, Phys. Rev. **32**, 6582 (1985).

[13]L. P. Gorkov, Sov. Phys.—JETP **59**, 1057 (1984) [Zh. Eksp. Teor. Fiz. **86**, 1818 (1984)].

[14]B. Horovitz, H. Gutfreund, and M. Weger, Phys. Rev. B **12**, 3174 (1975).

[15]V. N. Popov, Sov. Phys.—JETP **37**, 341 (1973) [Zh. Eksp. Teor. Fiz. **64**, 672 (1973)].

[16]M. E. Peskin, Ann. Phys. (N.Y.) **113**, 122 (1978).

[17]H. Kleinert, Phys. Lett. **93A**, 86 (1982); *Gauge Fields in Condensed Matter* (World Scientific, Singapore, 1989).

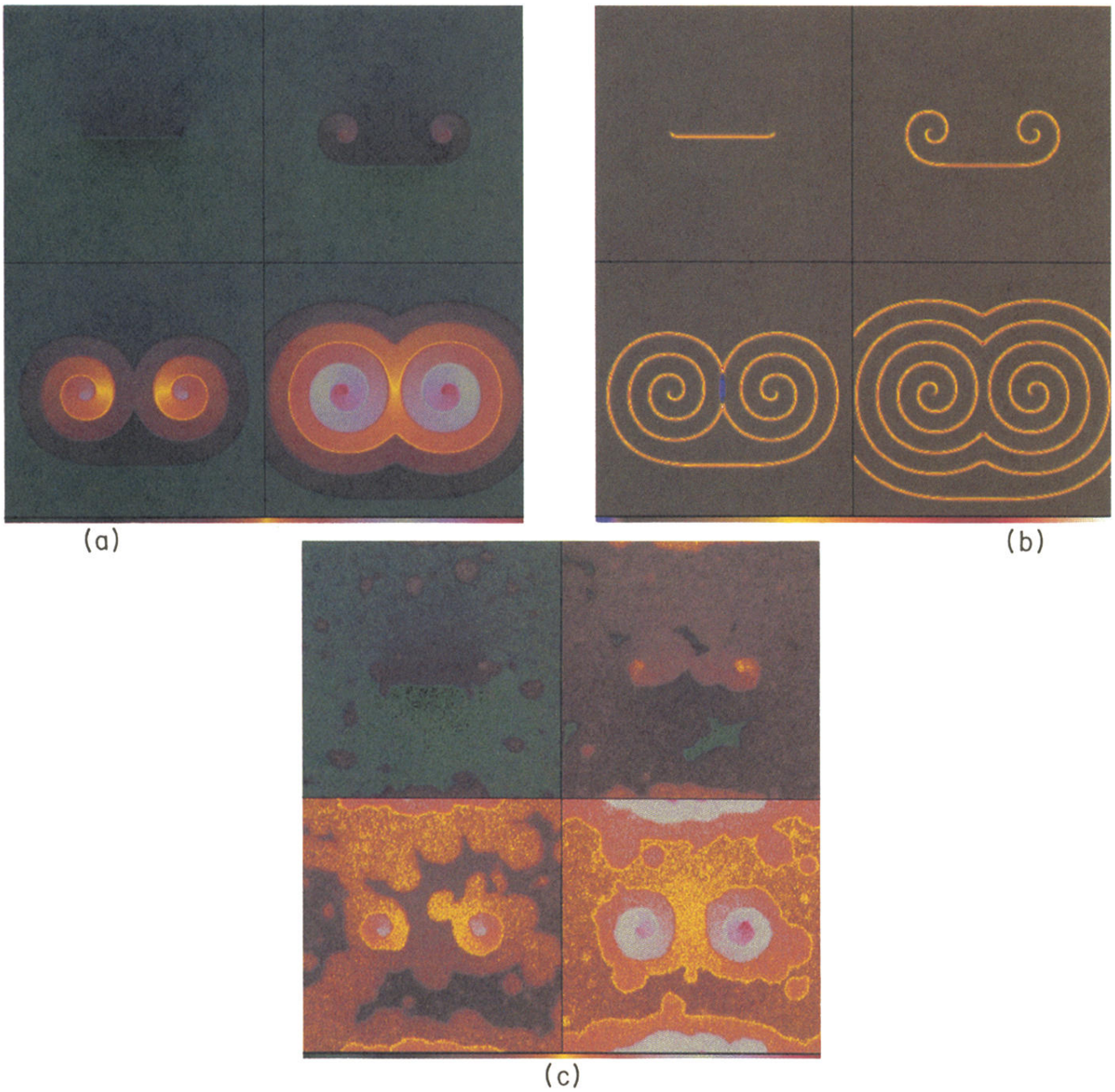

FIG. 1. Snapshots from the time evolution of two counter rotating spirals (a Frank-Read source). Panels (a), where $I=0.8$, $\epsilon=1.0$, and $T=0$, show ϕ for four different time snapshots. Panels (b) show the growth rate $\dot{\phi}$ for the same parameter values. Finally panels (c) show the growth of ϕ at a finite temperature just below the crossover to nucleation dominated growth ($I=0.65$, $\epsilon=1.0$, and $T=1.0$). Note in addition to the spiral a large nucleation cluster near the (periodic) boundary. The times are the same as for panels (a) and (b). The color bar at the bottom of each panel gives the magnitude of the growth (growth rate) increasing from left to right.